



Association of Brain Iron Overload With Brain Edema and Brain Atrophy After Intracerebral Hemorrhage

Ran Liu¹, Haoran Zhang¹, Shuangjuan Cheng², Yuyao Sun¹, Haijiao Li², Jiangxi Xiao^{2*} and Yining Huang^{1*}

¹ Department of Neurology, Peking University First Hospital, Beijing, China, ² Department of Radiology, Peking University First Hospital, Beijing, China

OPEN ACCESS

Edited by:

Yuhua Fan,
First Affiliated Hospital of Sun Yat-sen
University, China

Reviewed by:

Bo Gao,
Affiliated Hospital of Guizhou Medical
University, China
Mark S. Bolding,
University of Alabama at Birmingham,
United States

*Correspondence:

Jiangxi Xiao
cjr.xiaojiangxi@vip.163.com
Yining Huang
ynhuang@bjmu.edu.cn

Specialty section:

This article was submitted to
Applied Neuroimaging,
a section of the journal
Frontiers in Neurology

Received: 03 September 2020

Accepted: 20 November 2020

Published: 18 December 2020

Citation:

Liu R, Zhang H, Cheng S, Sun Y, Li H,
Xiao J and Huang Y (2020)
Association of Brain Iron Overload
With Brain Edema and Brain Atrophy
After Intracerebral Hemorrhage.
Front. Neurol. 11:602413.
doi: 10.3389/fneur.2020.602413

Objective: This study evaluated iron overload after intracerebral hemorrhage (ICH) using ESWAN sequences.

Methods: This single-center prospective observational cohort study enrolled supratentorial ICH patients. MRI was obtained with a 3.0-T scanner at day 1, day 14, day 30, and follow-up (300 days or later). R2* mapping was generated based on the ESWAN. R2* value of the ipsilateral side represented iron deposition, and the R2* value of the contralateral side served as control. R2* value was adjusted by volume and used to assess total iron overload. Brain edema was measured on T2 FLAIR-weighted images. Brain atrophy was calculated as the contralateral hemisphere volume minus the injured hemisphere volume.

Results: Twenty-seven patients with a spontaneous supratentorial ICH were included in this analysis. The ipsilateral R2* value was 40.27 ± 11.62 , 41.92 ± 13.56 , and 60.89 ± 14.09 at days 1, 14, and 30, respectively. The R2* value was significantly higher in the ICH side than the contralateral side ($p < 0.01$). Increased R2* value was seen on day 30 compared to day 14 ($p < 0.01$). The R2* value showed logistic decay with the distance to the hematoma margin ($p < 0.01$). Brain edema at day 14 and brain atrophy at follow-up correlated with R2* value adjusted by volume at day 14 ($p < 0.01$).

Conclusions: After ICH, the iron deposition in the perihematoma region was progressively increased during the first month. R2* value adjusted by volume predicted acute brain edema and chronic brain atrophy.

Keywords: cerebral hemorrhage, magnetic resonance imaging, iron overload, susceptibility weighted image (SWI), brain edema

INTRODUCTION

Intracerebral hemorrhage (ICH) is a devastating disease with high morbidity and mortality (1). The rupture of a large number of erythrocytes in a hematoma leads to the mass accumulation of hemoglobin, which causes the accumulation of iron in the hematoma and surrounding tissue and subsequently results in iron overload (2). Iron overload provokes a neurotoxic effect and is causally related to edema formation after ICH and delayed neuronal injury (3, 4). In clinical studies, the level of ferritin on admission is associated with poor outcome in patients with ICH (5–7). In animal models, iron chelator has been shown to reduce ICH-induced brain edema, neuronal death,

brain atrophy, and neurological deficits (8, 9). A randomized controlled trial revealed that iron chelator is safe but the efficacy of this needs further study (10, 11). To interpret the effects of such interventions, a full understanding of the natural history and clinical significance of iron overload is needed.

A hematoma contains deoxyhemoglobin and hemosiderin, from which the susceptibility effects cause signal decay, resulting in a hypointense signal on T2*-weighted magnetic resonance imaging (MRI) (12). Susceptibility weighted imaging (SWI) has been shown to have a higher sensitivity for detecting iron than conventional T2*-weighted MRI. Furthermore, R2*, the reciprocal of T2*, is near-linear rise with iron concentration, and R2* mapping could estimate perihematomal brain iron content in the rat ICH model (13). However, there remains a lack of studies that detect iron overload in ICH patients using MRI.

Therefore, we aimed to quantify the iron overload in the perihematomal area using SWI during the first 30 days after intracerebral hemorrhage, and investigate the relationship between iron concentration with acute brain edema and chronic brain atrophy.

METHODS

Subjects

The design of the study has been previously published (14). This study was a single-center prospective observational cohort study enrolling ICH patients. The study was approved by the ethics committee of Peking University Health Science Center and Michigan University Joint Institute, and informed consent was obtained from the patients or their surrogates.

Inclusion and Exclusion Criteria

The study included consecutive men and non-pregnant women >18 years old with a primary supratentorial hematoma, admitted within 24 h after symptom onset. The detailed exclusion criteria have been previously published (14).

Clinical Assessments

Demographic data, vascular risk factors, and clinical characteristics were prospectively collected. The modified Boston criteria were used to assess possible/probable cerebral amyloid angiopathy (CAA) on MRI scans. If cortical superficial siderosis and/or multiple cortical microbleeds, or a single lobar hemorrhage, were present, patients were classified as “probable CAA” (15, 16). At their follow-up visit, cognitive function was evaluated with the Mini-mental State Examination (MMSE) and Montreal Cognitive Assessment (MoCA).

Imaging Protocol

All patients underwent non-contrast head computed tomography (CT) on admission. MRI was performed on a GE Discovery MR750 3.0-T scanner at day 1 (24 ± 12 h), day 14 (14 ± 3 days), day 30 (3–6 weeks), and follow-up (300 days or later). All ESWAN sequences were acquired using a 3D-enhanced T2* susceptibility-weighted angiography contrast flow compensated multiecho gradient echo sequence, which was performed with the following parameters: repetition time (TR)

22.7 ms, echo time (TE) 3.2/5.6/7.9/10.3/12.6/15.0/17.3/19.7 ms, and slice thickness 2 mm. The parameters of routine MR imaging were as follows: T1 weighted images (T1WI): TR 1750 ms, TE 25 ms; T2 weighted images (T2WI): TR 5,092 ms, TE 92.5 ms; T2 Fluid Attenuated Inversion Recovery (T2-FLAIR): TR 8,400 ms, TE 150 ms; and T2* weighted images (T2*WI): TR 300 ms, TE 7.7 ms. These routine sequences were acquired with 5-mm-thick contiguous sections.

Image Analysis

The initial hematoma volume was measured based on the admission CT using the ABC/2 method. Using postprocessor software (ESWAN software, GE), magnitude images and high-pass filtered phase images were automatically presented, which were transformed to pseudocolor images and achieved R2* images. The R2* region of interests (ROIs) with an area of 1 mm² were acquired on the section with the largest hematoma. Edge of hematoma was defined on SWI image. Ipsilateral R2* ROIs were drawn along the edge of the hematoma on R2* images, and the mirrored area in the contralateral hemisphere served as the intraindividual control (**Figure 1A**). The number of ROIs varied according to the size of the hematoma. For the hemorrhagic side, 9.35 ± 1.37 ROIs were made on day 1, 7.82 ± 2.04 ROIs were made on day 14, and 8.33 ± 1.80 ROIs were made on day 30. 4 ROIs were made on the contralateral side at each time point. Each ipsilateral and contralateral R2* value was measured and then averaged to obtain a final value. All R2* values were measured by two neurologists (Dr. Ran Liu and Dr. Haoran Zhang), the interrater correlation coefficients were 0.910 (95% CI, 0.844–0.948) for ipsilateral R2* value and 0.947 (95% CI, 0.911–0.969) for contralateral R2* value.

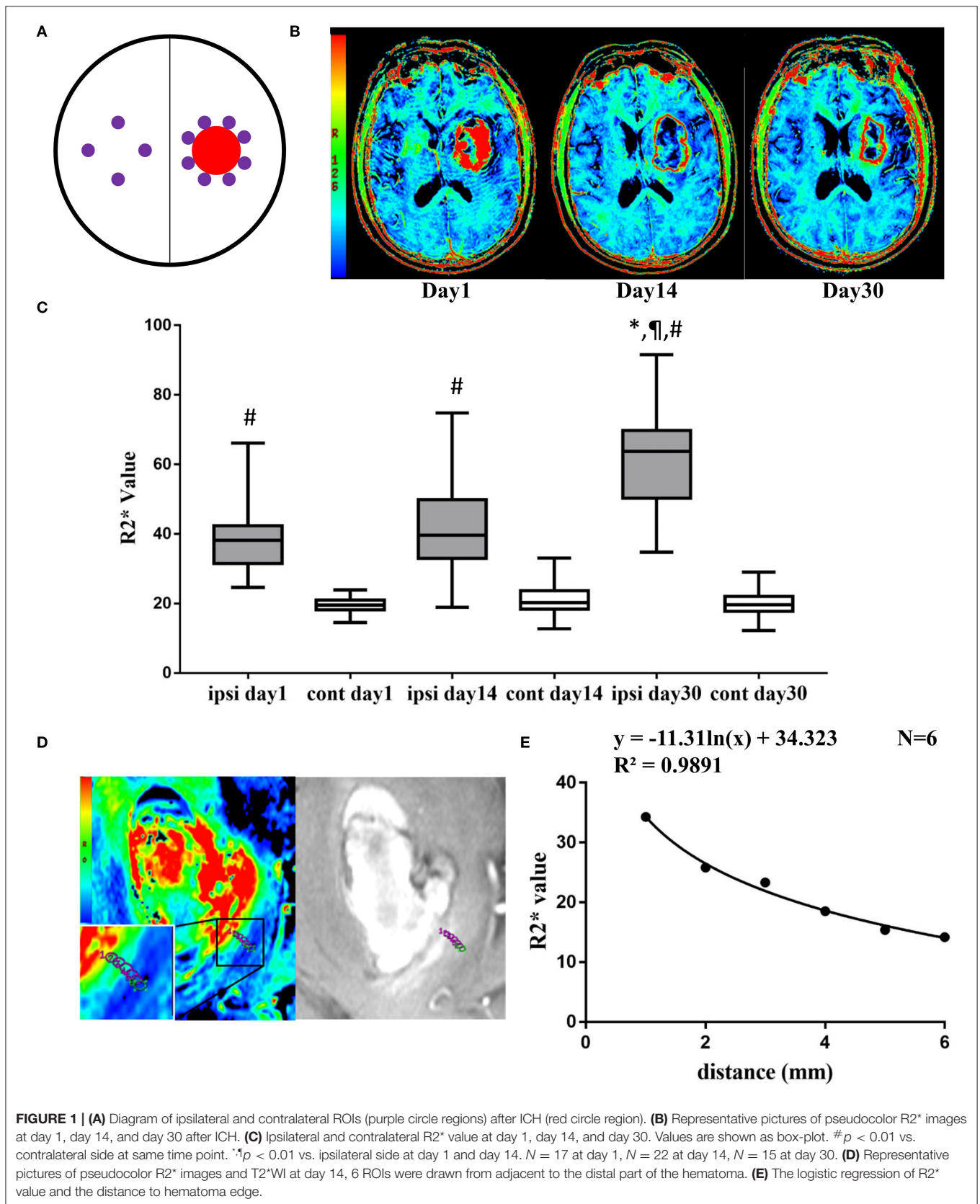
To investigate the distribution of R2* value in the perihematomal area, ROIs were set perpendicular to the edge of the hematoma. Six ROIs were placed adjunctive to the hematoma continuously from adjacently to distally, and the R2* value of each was measured (**Figure 1D**).

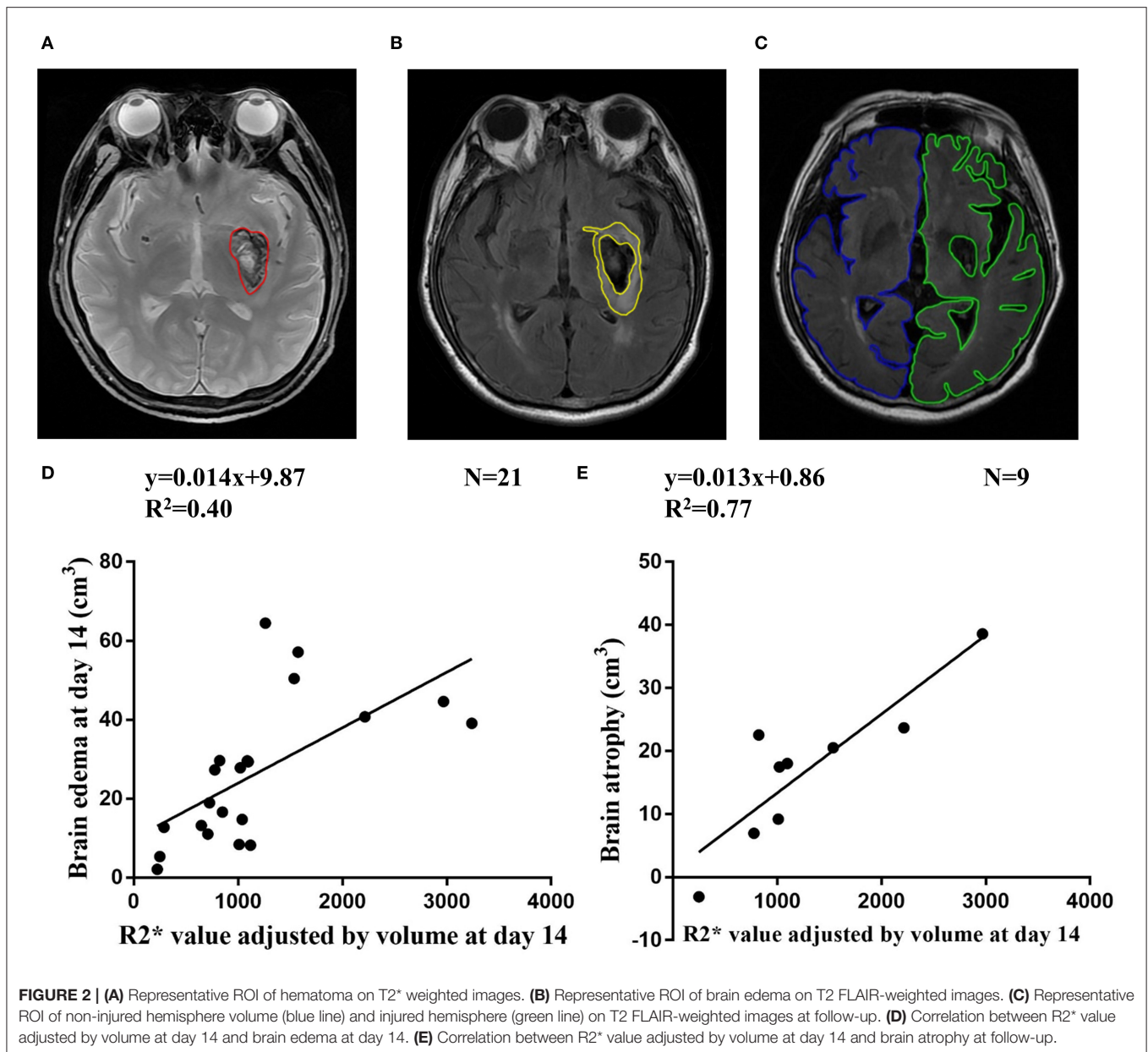
T2*WI and T2 FLAIR images were analyzed with MRICro version 1.40. Hematoma were outlined on T2*WI images on day 1, day 14, and day 30 (**Figure 2A**). Brain edema was drawn on T2 FLAIR-weighted images as total lesions minus hematoma lesions (**Figure 2B**). Hemisphere volume was drawn on T2 FLAIR-weighted images excluding areas of ventricles and damage at follow-up (17). Brain atrophy volume was calculated as the non-injured hemisphere volume minus the injured hemisphere volume (**Figure 2C**).

We assumed that the hematoma was a sphere with radius (R), surface (S), and volume (V). Then we defined R2* value adjusted by volume = ipsilateral R2* value × S = 4.84 × V^{2/3} × ipsilateral R2* value.

Statistical Analysis

All statistical analyses were performed using the Statistical Program for Social Sciences (SPSS) statistical software (version 24.0). Categorical variables were shown as numbers and percentages. Continuous variables were expressed as the mean ± SD or median values and interquartile range as appropriate.





A paired *t*-test was applied to investigate the differences of R2* value between ipsilateral and contralateral sides. The R2* value of the ipsilateral side at different time points were compared with a paired *t*-test. A logistic regression model was used to test for correlations with distance and the corresponding R2* value. Relationships between the R2* value adjusted by volume and brain edema/brain atrophy were assessed with Spearman's correlation. According to the median of R2* value adjusted by volume, patients were divided into two groups. Chi-square test, non-parametric test, or *t*-test were used to compare characteristics between groups. A value of $P < 0.05$ was considered significant.

RESULTS

Patient Characteristics

A total of 30 patients with ICH were enrolled between January and November 2014. Three patients were excluded due to poor image quality. The demographic, clinical, laboratory, and radiological characteristics are shown in **Table 1**. None of the enrolled patients were on anticoagulating therapy before index ICH. All patients underwent a diagnostic CT scan on day 1. Blood pressure was continuously monitored and carefully managed. The systolic blood pressures were <160 mmHg when the first MRI was taken and 140 mmHg when the rest of the MRI were taken. In total, 17, 22, and 15 patients underwent MRI on day

TABLE 1 | Demographic and clinical data for all patients ($N = 27$).

Demographic data	
Age, y	59.59 ± 12.19
Male, No. (%)	23 (85.20%)
Medical history, No. (%)	
Hypertension	19 (70.40%)
Diabetes	5 (18.50%)
Intracerebral hemorrhage	2 (7.40%)
Smoking	14 (51.90%)
Etiology of ICH, No. (%)	
Hypertension	17 (62.96%)
Cerebral amyloid angiopathy	2 (7.40%)
Unknown	8 (29.62%)
Admission clinical data	
Glasgow Coma Scale score	15.00 (1.00)
NIHSS score	7.00 ± 4.01
Systolic blood pressure, mm Hg	159.78 ± 26.95
Diastolic blood pressure, mm Hg	98.63 ± 16.12
Imaging data	
Lobar location of ICH, No. (%)	5 (18.50%)
Deep location of ICH, No. (%)	22 (81.50%)
Hematoma volume on admission CT, cm ³	14.46 ± 7.83
Brain edema volume at day 1, cm ³	17.69 ± 9.65
Brain edema volume at day 14, cm ³	26.25 ± 17.71
Brain edema volume at day 30, cm ³	9.76 ± 10.61
Brain atrophy volume at follow-up, cm ³	13.43 ± 12.49
Laboratory data	
Leukocyte, 10 ⁹ /L	6.93 ± 1.71
Hemoglobin, g/L	148.00 (22.00)
Platelets, 10 ¹² /L	196.30 ± 42.55
Glucose, mmol/L	6.15 (1.47)
TCHO, mmol/L	4.64 (0.77)
TG, mmol/L	1.29 (0.94)
LDL, mmol/L	2.80 ± 0.79
HDL, mmol/L	1.03 (0.36)
Creatinine, μmol/L	90.59 ± 13.31
PT, s	10.30 (1.15)
INR	1.00 (0.09)
Homocysteine, mmol/L	18.95 (17.26)
Treatment, No. (%)	
Mannitol	24 (88.89%)
Glycerol fructose	6 (22.22%)
Intravenous antihypertensive drugs	2 (7.40%)
Oral antihypertensive drugs	18 (66.67%)
3-month outcome	
Mortality, No. (%)	0 (0%)
Modified rankin score	2.00 (1.00)

1, day 14 and day 30, respectively. Fifteen patients underwent follow-up MRI, but three patients were excluded because of bilateral ICH, history of cerebral infarction, or new stroke after enrollment.

MRI Quantification of Iron Overload in ICH Patients

On day 1, the highest R2* region remained inside the hematoma. At day 14, the highest R2* region was located mainly in the perihematomal area, showing a red ring surrounding the hematoma. In the T2 FLAIR-weighted sequence, there was remarkable edema in the perihematomal region. At day 30, the edema remitted, and there was a clear area of red signal in the area surrounding the hematoma (**Figure 1B**).

The ipsilateral R2* value was 40.27 ± 11.62, 41.92 ± 13.56, and 60.89 ± 14.09 at day 1, 14, and 30, respectively (**Figure 1C**). The contralateral R2* value was 19.59 ± 2.34 at day 1, 21.16 ± 4.37 at day 14, and 19.76 ± 4.00 at day 30 (**Figure 1C**). The R2* value was significantly higher in the ipsilateral side than the contralateral side at day 1 ($t = 7.17$, $df = 16$, $p < 0.01$), day 14 ($t = 6.92$, $df = 21$, $p < 0.01$), and day 30 ($t = 12.88$, $df = 14$, $p < 0.01$). The R2* value at day 30 was significantly greater than day 1 ($t = 4.14$, $df = 6$, $p < 0.01$) and day 14 ($t = 5.93$, $df = 11$, $p < 0.01$) (**Figure 1C**).

At day 14, the R2* value decreased from 34.28 to 14.18 within 5 mm of distance. There was a logistic decay of R2* value in the perihematomal area from adjacent to the distal location ($R^2 = 0.99$, $n = 6$, $p < 0.01$) (**Figure 1E**).

The Relationship Between R2* Value Adjusted by Volume With Brain Edema, Brain Atrophy, Demographic Data, Vascular Risk Factors, and Clinical Characteristics

The brain edema volume was 17.69 ± 9.65 cm³, 26.25 ± 17.71 cm³, 9.76 ± 10.61 cm³ at day 1, day 14, and day 30, respectively. At day 1 and day 14, R2* value adjusted by volume was correlated with brain edema ($R^2 = 0.30$, $n = 15$, $p = 0.03$ and $R^2 = 0.40$, $n = 21$, $p < 0.01$, respectively) (**Figure 2D** and **Supplementary Figure 1A**). At day 30, the correlation between R2* value adjusted by volume and brain edema was not significant ($R^2 = 0.26$, $n = 14$, $p = 0.06$) (**Supplementary Figure 1C**).

Of the 12 patients who had MRI at follow up, brain volume was 13.43 ± 12.49 cm³. The MMSE and MoCA scores at follow-up were 29.50 ± 0.80 and 27.33 ± 2.10, respectively. The R2* value was adjusted by volume at day 14 and correlated with brain atrophy at follow-up ($R^2 = 0.77$, $n = 9$, $p < 0.01$) (**Figure 2E**). The correlation between R2* value was adjusted by volume at day1/day30 and brain atrophy was not significant (**Supplementary Figures 1B,D**).

There was a significant difference of age ($p = 0.029$) and initial hematoma volume ($p < 0.01$) between the high and low R2* value adjusted by volume groups (**Table 2**).

DISCUSSION/CONCLUSION

In this study, we aimed to validate the dynamic assessment of brain iron concentrations in perihematomal tissue after ICH with MR imaging. There were several major findings in the current study: (1) the iron concentration in the perihematomal region was progressively increased during the first month after ICH; and

TABLE 2 | Relationships of R2* value adjusted by volume and clinical data (N = 21).

	Low R2* value adjusted by volume group (N = 10)	High R2* value adjusted by volume group (N = 11)	P
Demographic data			
Age, y	63.70 ± 8.06	54.27 ± 9.99	0.029*
Male, No. (%)	8 (80.00%)	10 (90.91%)	0.476
Medical history, No. (%)			
Hypertension	8 (80.00%)	7 (63.64%)	0.407
Diabetes	1 (10.00%)	4 (36.36%)	0.157
Smoking	7 (70.00%)	6 (54.55%)	0.466
Admission clinical data			
Glasgow Coma Scale score	15.00 (5.00)	15.00 (1.00)	0.863
NIHSS score	8.10 ± 5.07	6.18 ± 2.56	0.280
Systolic blood pressure, mm Hg	167.60 ± 32.03	158.45 ± 23.92	0.465
Diastolic blood pressure, mm Hg	96.90 ± 12.74	102.64 ± 16.39	0.385
Imaging data			
Lobar location of ICH, No. (%)	3 (30.00%)	1 (9.09%)	0.223
Hematoma volume on admission CT, cm ³	10.19 ± 5.10	18.37 ± 7.44	0.009**
Laboratory data			
Leukocyte, 10 ⁹ /L	6.58 ± 1.46	7.19 ± 2.07	0.450
Hemoglobin, g/L	142.50 (32.00)	150.00 (23.00)	0.557
Platelets, 10 ¹² /L	192.20 ± 48.78	190.91 ± 43.27	0.949
Glucose, mmol/L	5.44 (1.67)	6.37 (2.29)	0.099
TCHO, mmol/L	4.47 (1.42)	4.79 (1.01)	0.173
TG, mmol/L	1.00 (0.94)	1.61 (1.05)	0.061
LDL, mmol/L	2.43 ± 0.72	2.81 ± 0.67	0.218
HDL, mmol/L	1.20 (0.39)	1.01 (0.53)	0.223
Creatinine, μmol/L	90.01 ± 6.88	92.04 ± 18.54	0.749
PT, s	10.30 (0.88)	10.40 (1.40)	0.912
INR	1.02 (0.11)	1.00 (0.12)	0.573
Homocysteine, mmol/L	28.89 (39.65)	15.19 (10.45)	0.142
3-month outcome			
Modified rankin score	2.00 (0.75)	2.00 (1.00)	0.349

p* < 0.05, *p* < 0.01.

(2) the brain edema in the acute stage and brain atrophy in the later stage correlated with brain iron overload after ICH.

In the current study, the iron concentration in the perihematoma region began to increase within 24 hours after ICH. At day 1, the iron concentration was about 2 times more than the contralateral side. It continued to progress in the first month. At day 30, the iron concentration was approximately 3 times more than the contralateral side. In a rat model of ICH, the iron content reached its maximum at day 14 and was 2 times greater than the contralateral side (13). In comparison with the animal model, iron overload was more prominent and lasted longer than in human patients. Although the R2* value reached its maximum during the last scan, iron accumulation may still be ongoing afterward. Therefore, further investigations are needed to identify the peak time and time course of iron accumulation. When translating iron chelating therapy from an animal model to a human one, species difference should be considered, and the treatment course may be expanded to achieve a better effect.

There has been a continuous effort to explore a method for decreasing secondary injury and improving the prognosis of ICH. For example, deferoxamine has been shown to reduce brain injury by attenuating brain edema (9). The quantification of iron overload provides useful information in defining the therapeutic time window and the optimal duration of these treatments. Although quantitative susceptibility mapping (QSM) is more accurate for iron quantification (18), SWI is a widely available sequence and can be used in the routine clinical evaluation of iron overload after ICH.

In this study, we did not find a significant increase in ipsilateral R2* values from day 1 to day 14. Both the pseudocolor image and the R2* values showed that the evaluation of iron concentration was greatly influenced by the distinguished brain edema in ICH patients. When measured by serial MRI, perihematoma edema (PHE) was progressive and reached its maximum 14 days after onset. The development of PHE probably resulted in the plateau of R2* value from day 1 to day 14. Although the R2* value

is strongly affected by iron concentration, the water content of brain tissue can also influence the $R2^*$ value.

The $R2^*$ value showed logistic decay in the perihematomal area. On the fourteenth day after ICH, the $R2^*$ value decreased from 34.28 to 14.18 in 5 mm of distance. This region manifested the migration of iron overload and the accumulation of hemosiderin in the perihematomal area, which represented the vulnerable tissue and secondary injury after ICH. The migration of iron can be visualized in ESWAN images from the hematoma to the perihematomal region. The highest iron concentration was located mainly inside the hematoma on day 1. At this stage, iron was mostly stored in red blood cells, and hemoglobin as erythrocyte lysis begins. During this period, iron was mainly stored as ferritin and hemosiderin (19). Previous studies indicate that ferritin reached its maximum on days 7 to 14 after ICH (20, 21), while hemosiderin began to accumulate 6 days after ICH (22). Therefore, hemosiderin may be the major protein responsible for iron measurement at later stages.

In the current study, we defined $R2^*$ value adjusted by volume, a new indicator of perihematomal iron overload. In the previous $FeCl_2$ infusion ICH experiment, simply iron overload resulted in acute brain edema and chronic brain tissue loss (23). However, there were few non-invasive methods to measure iron overload in ICH patients in the past, e.g., serum ferritin level. The current study indicated that $R2^*$ value adjusted by volume may be a marker of iron overload and a predictor of brain edema and atrophy. In this study, we used the volume difference between the two hemispheres as tissue loss, which can partially offset normal aging atrophy. In addition, the median atrophy rate of normal subjects was approximately -0.38% per year (24), which can be neglected compared to ICH injury.

Some limitations of the study must be noted. (1) The location of hematomas varies in our study. Although most of the hematomas were located in the basal ganglia, there were some patients with lobar hemorrhage. Iron accumulation in different brain structures is different as a consequence of normal aging. Additionally, $R2^*$ values are influenced by the myelin content in the brain (25). The heterogeneity of clinical characteristics should be considered when analyzing the results in this study. (2) Age-related differences in iron deposition in the brain are region specific. The basal ganglia were the location where the $R2^*$ value was greatly related to older age (26). In our cohort, the age of all patients ranged from 37 to 83 years old. Therefore, the iron deposition caused by aging cannot be excluded, although the dynamic change in iron overload was mainly due to the

degradation of hemoglobin released from the hematoma. (3) Our study is also limited due to the small sample size.

In conclusion, the iron concentration in the perihematomal region progressively increased during the first month after ICH. $R2^*$ value adjusted by volume may be a predictor of brain edema and atrophy.

DATA AVAILABILITY STATEMENT

The original contributions presented in the study are included in the article/**Supplementary Materials**, further inquiries can be directed to the corresponding authors.

ETHICS STATEMENT

The study was approved by the ethics committee of Peking University Health Science Center and Michigan University Joint Institute, and informed consent was obtained from the patients or their surrogates.

AUTHOR CONTRIBUTIONS

RL contributed to the acquisition of data, data analysis, and interpretation. HZ contributed to data analysis, interpretation, and manuscript preparation. SC contributed to the acquisition of data and revision of the manuscript. YS and HL contributed to the acquisition of data and data analysis. JX contributed to study concept and design, image analysis, and interpretation. YH contributed to study concept, design, and supervision. All authors contributed to the article and approved the submitted version.

FUNDING

This study was supported by grants from the UMHS-PUHSC Joint Institute (BMU20140472) and grants from the National Natural Science Foundation of China (81701148).

SUPPLEMENTARY MATERIAL

The Supplementary Material for this article can be found online at: <https://www.frontiersin.org/articles/10.3389/fneur.2020.602413/full#supplementary-material>

Supplementary Figure 1 | (A,C) Correlation between $R2^*$ value adjusted by volume and brain edema at day 1 **(A)** and day 30 **(D)**. **(B,D)** Correlation between $R2^*$ value adjusted by volume at day 1 **(B)**/day 30 **(D)** and brain atrophy at follow-up.

REFERENCES

- Keep RF, Hua Y, Xi G. Intracerebral haemorrhage: mechanisms of injury and therapeutic targets. *Lancet Neurol.* (2012) 11:720–31. doi: 10.1016/S1474-4422(12)70104-7
- Siesjö BK, Agardh CD, Bengtsson F. Free radicals and brain damage. *Cerebrovasc Brain Metab Rev.* (1989) 1:165–211.
- Xi G, Strahle J, Hua Y, Keep RF. Progress in translational research on intracerebral hemorrhage: is there an end in sight? *Prog Neurobiol.* (2014) 115:45–63. doi: 10.1016/j.pneurobio.2013.09.007
- Hua Y, Keep RF, Hoff JT, Xi G. Brain injury after intracerebral hemorrhage: the role of thrombin and iron. *Stroke.* (2007) 38(2 Suppl.):759–62. doi: 10.1161/01.STR.0000247868.97078.10

5. Pérez de la Ossa N, Sobrino T, Silva Y, Blanco M, Millán M, Gomis M, et al. Iron-related brain damage in patients with intracerebral hemorrhage. *Stroke*. (2010) 41:810–3. doi: 10.1161/STROKEAHA.109.570168
6. Mehdiratta M, Kumar S, Hackney D, Schlaug G, Selim M. Association between serum ferritin level and perihematoma edema volume in patients with spontaneous intracerebral hemorrhage. *Stroke*. (2008) 39:1165–70. doi: 10.1161/STROKEAHA.107.501213
7. Yang G, Hu R, Zhang C, Qian C, Luo QQ, Yung WH, et al. A combination of serum iron, ferritin and transferrin predicts outcome in patients with intracerebral hemorrhage. *Sci Rep*. (2016) 6:21970. doi: 10.1038/srep21970
8. Hua Y, Nakamura T, Keep RF, Wu J, Schallert T, Hoff JT, et al. Long-term effects of experimental intracerebral hemorrhage: the role of iron. *J Neurosurg*. (2006) 104:305–12. doi: 10.3171/jns.2006.104.2.305
9. Nakamura T, Keep RF, Hua Y, Schallert T, Hoff JT, Xi G. Deferoxamine-induced attenuation of brain edema and neurological deficits in a rat model of intracerebral hemorrhage. *J Neurosurg*. (2004) 100:672–8. doi: 10.3171/jns.2004.100.4.0672
10. Selim M, Yeatts S, Goldstein JN, Gomes J, Greenberg S, Morgenstern LB, et al. Safety and tolerability of deferoxamine mesylate in patients with acute intracerebral hemorrhage. *Stroke*. (2011) 42:3067–74. doi: 10.1161/STROKEAHA.111.617589
11. Selim M, Foster LD, Moy CS, Xi G, Hill MD, Morgenstern LB, et al. Deferoxamine mesylate in patients with intracerebral haemorrhage (i-DEF): a multicentre, randomised, placebo-controlled, double-blind phase 2 trial. *Lancet Neurol*. (2019) 18:428–38. doi: 10.1016/S1474-4422(19)30069-9
12. de Champfleury NM, Langlois C, Ankenbrandt WJ, Le Bars E, Leroy MA, Duffau H, et al. Magnetic resonance imaging evaluation of cerebral cavernous malformations with susceptibility-weighted imaging. *Neurosurgery*. (2011) 68:641–7; discussion: 7–8. doi: 10.1227/NEU.0b013e31820773cf
13. Cao S, Hua Y, Keep RF, Chaudhary N, Xi G. Minocycline effects on intracerebral hemorrhage-induced iron overload in aged rats: brain iron quantification with magnetic resonance imaging. *Stroke*. (2018) 49:995–1002. doi: 10.1161/STROKEAHA.117.019860
14. Liu R, Li H, Hua Y, Keep RF, Xiao J, Xi G, et al. Early Hemolysis Within Human Intracerebral Hematomas: an MRI Study. *Transl Stroke Res*. (2019) 10:52–6. doi: 10.1007/s12975-018-0630-2
15. Knudsen KA, Rosand J, Karluk D, Greenberg SM. Clinical diagnosis of cerebral amyloid angiopathy: validation of the Boston criteria. *Neurology*. (2001) 56:537–9. doi: 10.1212/wnl.56.4.537
16. Linn J, Halpin A, Demaerel P, Ruhland J, Giese AD, Dichgans M, et al. Prevalence of superficial siderosis in patients with cerebral amyloid angiopathy. *Neurology*. (2010) 74:1346–50. doi: 10.1212/WNL.0b013e3181dad605
17. MacLellan CL, Silasi G, Poon CC, Edmundson CL, Buist R, Peeling J, et al. Intracerebral hemorrhage models in rat: comparing collagenase to blood infusion. *J Cereb Blood Flow Metab*. (2008) 28:516–25. doi: 10.1038/sj.jcbfm.9600548
18. Zhang Y, Wei H, Sun Y, Cronin MJ, He N, Xu J, et al. Quantitative susceptibility mapping (QSM) as a means to monitor cerebral hematoma treatment. *J Magn Reson Imaging*. (2018) 48:907–15. doi: 10.1002/jmri.25957
19. Thulborn KR, Sorensen AG, Kowall NW, McKee A, Lai A, McKinstry RC, et al. The role of ferritin and hemosiderin in the MR appearance of cerebral hemorrhage: a histopathologic biochemical study in rats. *AJNR Am J Neuroradiol*. (1990) 11:291–7.
20. Wu J, Hua Y, Keep RF, Nakamura T, Hoff JT, Xi G. Iron and iron-handling proteins in the brain after intracerebral hemorrhage. *Stroke*. (2003) 34:2964–9. doi: 10.1161/01.STR.0000103140.52838.45
21. Wang G, Hu W, Tang Q, Wang L, Sun XG, Chen Y, et al. Effect comparison of both iron chelators on outcomes, iron deposit, and iron transporters after intracerebral hemorrhage in rats. *Mol Neurobiol*. (2016) 53:3576–85. doi: 10.1007/s12035-015-9302-3
22. Koeppen AH, Dickson AC, McEvoy JA. The cellular reactions to experimental intracerebral hemorrhage. *J Neurol Sci*. (1995) 134(Suppl.):102–12. doi: 10.1016/0022-510X(95)00215-N
23. Caliaperumal J, Ma Y, Colbourne F. Intra-parenchymal ferrous iron infusion causes neuronal atrophy, cell death and progressive tissue loss: implications for intracerebral hemorrhage. *Exp Neurol*. (2012) 237:363–9. doi: 10.1016/j.expneurol.2012.07.001
24. Fjell AM, Walhovd KB, Fennema-Notestine C, McEvoy LK, Hagler DJ, Holland D, et al. One-year brain atrophy evident in healthy aging. *J Neurosci*. (2009) 29:15223–31. doi: 10.1523/JNEUROSCI.3252-09.2009
25. Möller HE, Bossoni L, Connor JR, Crichton RR, Does MD, Ward RJ, et al. Iron, myelin, and the brain: neuroimaging meets neurobiology. *Trends Neurosci*. (2019) 42:384–401. doi: 10.1016/j.tins.2019.03.009
26. Xu X, Wang Q, Zhang M. Age, gender, and hemispheric differences in iron deposition in the human brain: an in vivo MRI study. *NeuroImage*. (2008) 40:35–42. doi: 10.1016/j.neuroimage.2007.11.017

Conflict of Interest: The authors declare that the research was conducted in the absence of any commercial or financial relationships that could be construed as a potential conflict of interest.

Copyright © 2020 Liu, Zhang, Cheng, Sun, Li, Xiao and Huang. This is an open-access article distributed under the terms of the Creative Commons Attribution License (CC BY). The use, distribution or reproduction in other forums is permitted, provided the original author(s) and the copyright owner(s) are credited and that the original publication in this journal is cited, in accordance with accepted academic practice. No use, distribution or reproduction is permitted which does not comply with these terms.